

Marangoni flotation of liquid droplets

By R. SAVINO, D. PATERNA AND M. LAPPÀ

Università degli Studi di Napoli 'Federico II', Dipartimento di Scienza e Ingegneria dello Spazio 'Luigi G. Napolitano', P.le V.Tecchio 80, 80125 Napoli, Italy

(Received 25 June 2001 and in revised form 17 October 2002)

Flotation of liquid droplets on pool surfaces, in the presence of temperature differences, is studied experimentally and numerically. Coalescence or sinking of the droplet is prevented by the thermal Marangoni motion, owing to the surface tension imbalance at the pool surface. The mechanism is the same as that investigated in previous works on coalescence and wetting prevention in the presence of temperature differences. If the droplet is colder than the liquid surface, the flow is directed radially towards the drop; this radial flow field drags the ambient air under the drop, thus creating an air film and avoiding a direct contact between the droplet and the pool molecules.

The surface velocities are measured visually with a CCD camera to image the motion of tracers floating on the pool surface; the surface temperature distributions along the pool and the droplet surfaces are measured by an infrared thermocamera. The experimental results are correlated by numerical results obtained under the assumption of spherical drop and axisymmetric flow regime. Different liquids are considered and the influence of evaporation is discussed, showing a good agreement between the experiments and the numerical simulations.

1. Introduction

Flotation of liquid drops (e.g. water) over liquid surfaces can be traced back to Reynolds (1881) who mentioned floating droplets for the first time. When drops of water fall into water (e.g. rain drops or distillate water, etc.) they do not always coalesce immediately with the rest of the liquid, but remain on the pool surface for a certain time before disappearing (Walker 1978).

During kitchen activities there are many opportunities to deal with drops of different liquids (mainly water and oils) and there are chances to observe the 'strange' behaviour of drops that float, instead of spreading over the surface (if the droplet liquid is lighter than that of the pool) or of sinking (if the drop liquid is heavier than that of the pool). For instance, sometimes floating droplets are formed when oil is resupplied to a frying pan. In this case, typically, droplet flotation lasts a few seconds.

Many authors have tried to study this behaviour in isothermal conditions. Mahajan (1930*a, b*) investigated the conditions of non coalescence of falling droplets on the surface of the same liquid surrounded by different media. When air is the surrounding medium, they obtained controversial results and provided a number of speculative explanations. Nahmias, Tephany & Majanelle (1997) tried unsuccessfully to reproduce some of Mahajan's experiments. Walker (1978) assumes that the integrity of the floating droplet can be maintained, at least in part, by forces of electrical repulsion arising from the polarized nature of the liquid molecule. Experiments under low pressure have been carried out by Tephany & Nahmias (1999) to investigate the thinning of the air film separating the droplet from the pool liquid.

When thermal effects are negligible, in addition to possible electrostatic effects, surfactants play an important role. For instance, recently Amarouchene, Cristobal & Kellay (2001) report on experiments on 'long-lived' drops of surfactant solutions and explain the delay in the thinning of the air film on the basis of interfacial rheological properties (e.g. surface viscosity and surface elasticity). In this case, surface deformations cause surfactant concentration gradients giving rise to 'restoring' Marangoni stresses that are probably responsible for an extra resistance to the air flow drainage that delays coalescence (Gibbs–Marangoni effect). All the above experimental findings refer to possible concentration Marangoni effects; the present work refers to thermal Marangoni flows that will be briefly reviewed in the following.

The first articles dealing with non-coalescence induced by thermal Marangoni flow were published by Monti & Dell'Aversana (1994), and Dell'Aversana, Monti & Gaeta (1995) who present evidence of the unexpected phenomenon of suppression of coalescence, observed during the microgravity Spacelab D2 mission in April 1993, when two drops attached to two coaxial disks at different temperatures did not form a liquid bridge. Different explanations were initially proposed for the non-coalescence phenomenon: (i) a thin film of air between the two liquids owing to the Marangoni effect; (ii) a liquid–liquid interface with an interface tension, depending on the velocities of the liquids; (iii) electric repulsive charge; (iv) explanations in terms of thermal radiation forces.

Alterio (1994) and Lamanna (1994) tried to prove the air-film assumption. In this case, contrary to the other proposed physical mechanisms, the air film, responsible for the coalescence and wetting prevention, is due to surface tension unbalance (thermal Marangoni effect). More specifically, the ambient air is entrained between the two interfaces by the drop surface velocities and reaches pressures large enough to prevent coalescence and to balance the overpressure necessary to deform the drops.

Monti, Savino & Cicala (1995) formulated a fluid-dynamic model of non-coalescing liquid drops to explain the phenomenon of the air-film stability, in the presence of two counteracting driving actions along the surfaces of two drops (sessile and hanging) brought into contact in the presence of a temperature difference; their numerical results correlated with the experimental results on temperature differences, surface deformations, applied pressure and film thickness. The model was then extended and applied to the problem of wetting prevention of a hanging drop held by a circular disk and squeezed on a flat plate maintained at lower temperature (Monti, Savino & Tempesta 1998*b*) and to the non-coalescence of a hanging drop immersed in a pool of the same liquid (Monti *et al.* 1998*a*).

Dell'Aversana, Banavar & Koplik (1996) presented experimental results, molecular dynamics simulations (for the case of isothermal drops and applied shear stress) and a lubrication model, to explain the presence of the air film responsible for the non-coalescence. The air gap between the drop interface and the liquid bath is approximated assuming a stationary plate inclined at some angle over an infinite moving plate. For the non-isothermal case, the velocity of this plate is taken to be the characteristic Marangoni speed. Further experimental results on the subject have been performed by Dell'Aversana, Tontodonato & Carotenuto (1997) and Monti *et al.* (1998*b*), who studied independently the phenomenon of wetting prevention using laser interferometry, measuring the film thickness and its time evolution at different experimental conditions.

All these works deal with hanging drops held by a circular rod at controlled temperature. The behaviour of free droplets has been considered by Monti & Savino (1999, 2001) who carried out experiments with hot drops released on a cold solid

wall (the inverse calefaction effect). In the present paper, attention is focused on the case of a cold liquid droplet floating on a pool of warm liquid. Even though droplets floating over liquid surfaces, in the presence of temperature differences, were also mentioned by Monti & Dell'Aversana (1994) and Dell'Aversana & Neitzel (1998), no systematic experiments and no numerical simulations have been reported in the literature.

Experimental evidence suggests: (i) coalescence (for a drop and a liquid pool of the same liquid), (ii) spreading (for a drop of a wetting liquid lighter than the liquid pool), or (iii) sinking (for a drop of an immiscible liquid heavier than the liquid pool) are prevented by an overpressure in the air film between the droplet and the liquid interface, that balances the weight of the floating droplet at the upper side and depresses the pool surface at the lower side. This overpressure is induced by shear stresses due to the relative motion of the air flowing in the gap between the drop and the liquid surfaces (this is similar to what happens for the case of a hanging drop over a rotating pool (Dell'Aversana *et al.* 1996; Nahmias *et al.* 1997)) or in the case of a vibrating bath surface (S. Faez, personal communication 2000).

Even though the basic mechanism causing flotation of an isolated drop over a liquid pool at a different temperature is as explained in the above references (thermal Marangoni effect), there are substantial differences between the present and the previous works, as summarized below.

The problem under investigation is unsteady (full drop floating on a liquid bath) and refers to a different geometry and to different boundary conditions. A critical role is played by the heat transfer between the drop and the ambient and between the drop and the pool and, in some cases, by the drop evaporation. Attention is focused here on the case of a drop colder than the liquid pool; the driving action causing entrainment of the ambient air in the interstitial film between the liquid and the drop surface is in this case the thermal Marangoni flow at the pool surface, contrary to other problems previously investigated, e.g. the wetting prevention studied by Dell'Aversana *et al.* (1997) or by Monti *et al.* (1998*b*), where the driving action is the surface tension gradient along the drop surface. Since in the present problem the drop is colder than the liquid pool, the thermal Marangoni flow along the pool surface is directed radially inward; the Marangoni-driven flow caused by the air-drop interface is not an important part of this problem. Therefore, the flotation of a 'solid' sphere (or of a liquid drop that does not exhibit a Marangoni effect) on the same pool of liquid (for the same fluid dynamic mechanism) should be possible. Attempts are being made to find solid spheres of suitable density, roughness, thermal properties, size, that can float for a sufficient time over pool surfaces.

Since the mechanism responsible for the non-coalescence is the thermal Marangoni effect due to the surface temperature differences, an effort was made to measure the surface temperature distributions at the liquid interfaces. Accurate non invasive temperature measurement is made by an infrared thermograph; with this technique, it is possible to give an independent proof (in addition to the laser interferometry used in previous works) of the fact that the coalescence prevention is caused only by thermal Marangoni flows and not by other physical mechanisms (e.g. the dielectric property of silicone oils, see for instance Nahmias *et al.* 1997).

Compared to previous theoretical and numerical fluid dynamic models developed to correlate the experimental results (Monti *et al.* 1995; Monti & Savino 1996, 1997) this problem requires an unsteady numerical code able to perform the simultaneous solution of the fluid dynamic equations in the air film and in the liquid pool, in the droplet and in the surrounding ambient air (in the previous works the geometry

of the problem allowed us to assume simplified boundary conditions and steady calculations).

Furthermore, in the previous works, the pressure distribution in the air film was calculated under the assumptions of parallel and flat interstitial film either between two hemispherical drops squeezed one against the other (Monti *et al.* 1995; Monti & Savino 1996, 1997) or between a drop and a solid wall (Monti *et al.* 1998*b*). For a fully immersed hanging hemispherical drop (Monti *et al.* 1998*a*) a constant thickness air gap was assumed. For the problem under study (droplet floating on the surface of a liquid pool) the numerical correlations take into account the real shape of the liquid pool surface, which is strongly deformed by the weight of the drop.

2. Laboratory experiments

The experimental apparatus consists of a liquid pool (depth of only 5 mm to minimize buoyancy convection) whose temperature T_p can be regulated and controlled, by means of an external temperature bath, in a quiescent ambient air (at a temperature T_a). A droplet of the same liquid or of a different liquid is formed by a syringe and gently released over the pool surface. The temperatures of the droplet T_d and of the pool surface T_p are measured by an infrared thermocamera (Flir SC3000) operating in the long wave band (9 μm). The resolution of the thermocamera is 0.1 K and its sensitivity is 20 mK at 30 °C. The thermocamera has a standard 20° lens, but two additional close-up lens can be mounted to enlarge the field of view: with the first close-up lens, the field of view is $34 \times 25 \text{ mm}^2$ at 10 cm from the object; with the additional microscope lens, the field of view is $10 \times 7.5 \text{ mm}^2$ at a distance of 3 cm.

The position and size of the drop are also monitored by a CCD camera (top and lateral views); pool surface trajectories are observed by tracers floating over the bath. For the experiments presented in this paper, the pool liquid is a silicone oil with a kinematic viscosity of 3 cS and the droplets are of water or of silicone oils (100 cS or 1000 cS). Other bath liquids exhibit the same behaviour, albeit with less reproducibility. For instance, droplets of water, alcohol, acetyl-acetone, ethylene glycol and oils have been seen floating over pools of Fluorinert liquids, alcohols and silicone oils with different viscosities.

The situation is complicated when Marangoni effects are present both in the floating drop and in the pool liquid. Therefore, the present numerical analysis (§4) has been carried out in the simplest case in which Marangoni effects are negligible in the drop, i.e. with droplets of water or of viscous silicone oils. The physical properties of the liquids used are given in table 1. The silicone oil properties, in particular the surface tension (σ) and its derivative with temperature (σ_T), are provided by the Rhodorsil Huiles company.

It must be pointed out that, even though the temperature derivative of the surface tension of pure water reported in literature is $\sigma_T = 10^{-4} \text{ N m}^{-1} \text{ K}^{-1}$, this property is strongly dependent on the surface concentration of surfactants attracted by the surrounding ambient. In addition, experiments show that thermal Marangoni flows do not occur in water droplets, and this is generally also attributed to the properties of the water molecules that exhibit high attraction of impurities (surfactants).

In the present experiments, pure oils were used, but no special care was taken to avoid contamination of the water drops, since for the present configuration (cold drop and warm pool) the thermal Marangoni effect responsible for drop flotation arises at the pool–air interface. Because of the assumed absence of thermal Marangoni effects in water, a value of $\sigma_T = 0$ was assumed for all calculations that refer to water

	Water	Rhodorsil Huiles silicone oil 3 cS	Rhodorsil Huiles silicone oil 100 cS	Rhodorsil Huiles silicone oil 1000 cS
ρ (kg m ⁻³)	998.2	890	965	970
c_p (J kg ⁻¹ K ⁻¹)	4182	1970	1460	1460
λ (W m ⁻¹ K ⁻¹)	0.6	0.11	0.16	0.16
μ (kg m ⁻¹ s ⁻¹)	0.001	0.00265	0.0965	0.97
σ (N m ⁻¹)	0.07	0.019	0.0209	0.0211
σ_T (N m ⁻¹ K ⁻¹)	10 ⁻⁴ (zero for all calculations)	6 × 10 ⁻⁵	6 × 10 ⁻⁵	6 × 10 ⁻⁵

TABLE 1. Properties of the test liquids at reference conditions ($T_0 = 20^\circ\text{C}$).

droplets. Droplets of different sizes were examined (diameter ranging from 0.5 mm to 4 mm). Some pictures of floating droplets of different sizes (lateral view) are shown in figure 1. The pictures clearly indicate the pool surface deformation (larger for larger drops) near the droplets. A number of experiments have been carried out at different conditions.

2.1. Isothermal conditions

The droplet and the pool are at the same (ambient) temperature ($T_d = T_p = T_a \cong 25^\circ\text{C}$). In this case, the droplet immediately coalesces (for miscible liquids), sinks (for larger density immiscible liquid), or spreads over the surface (for lighter immiscible liquids).

2.2. Pool at temperature higher than that of the ambient

The temperature of the oil bath is larger than the ambient temperature (e.g. $T_p \cong 42^\circ\text{C}$) and the droplet is released at the ambient temperature ($T_d = T_a \cong 25^\circ\text{C}$). In this case the droplet, initially colder than the pool, remains floating over the oil surface. The thermocamera images show that the drop temperature increases with time, approaching the pool temperature, and the droplet remains floating until a small (critical) temperature difference exists (depending on the droplet liquid and size), after which coalescence or sinking occurs.

Figure 2 shows the thermographic images of a droplet of silicone oil (with kinematic viscosity of 100 cS) floating over a 3 cS silicone oil surface (the thermocamera is mounted vertically, above the pool surface). The diameter of the droplet is 3 mm. The initial temperature of the drop is equal to the ambient temperature ($T_d = T_a \cong 25^\circ\text{C}$); the pool is at temperature $T_p \cong 42^\circ\text{C}$. When the temperature difference between the droplet and the pool becomes less than about 2°C , the droplet coalesces with the pool liquid (after about 16 s).

The temperature profiles at different times along a surface line connecting the drop centre to the liquid pool (obtained from figure 2) are shown in figure 3. Figure 4 shows the corresponding temperature profiles of a droplet of water ($\rho_d \cong 1 \text{ g cm}^{-3}$), released over the same pool of silicone oil 3 cS ($\rho_p \cong 0.9 \text{ g cm}^{-3}$) at the same initial conditions. After an initial transient in which the drop temperature increases, a steady state is reached characterized by a temperature difference between the drop and the pool. In these conditions, the floating droplet stands over the pool surface for a ‘long’ time (at least longer than our observation) without sinking.

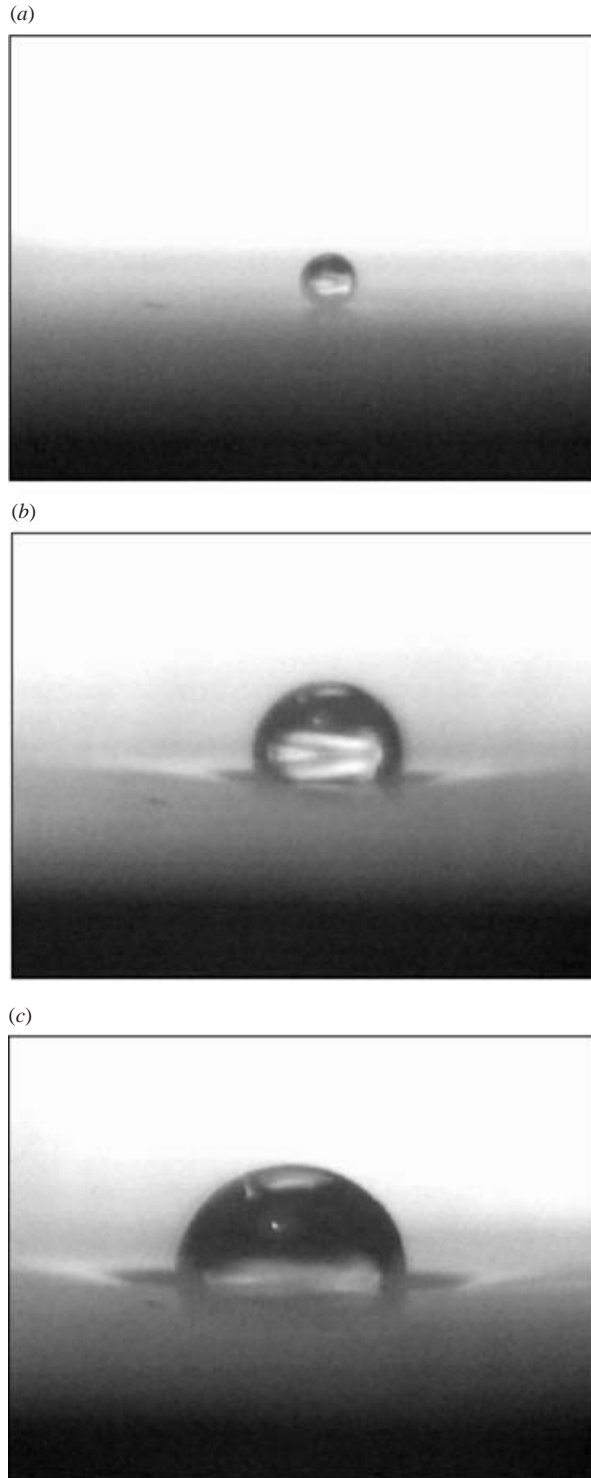


FIGURE 1. CCD images of drops of different diameters floating over a pool of silicone oil with kinematic viscosity of 3 cS. The pool temperature is 42 °C. The ambient temperature is 25 °C. The diameters of the drops are (a) $D = 0.82$ mm, (b) 2.25 mm, (c) 3.45 mm.

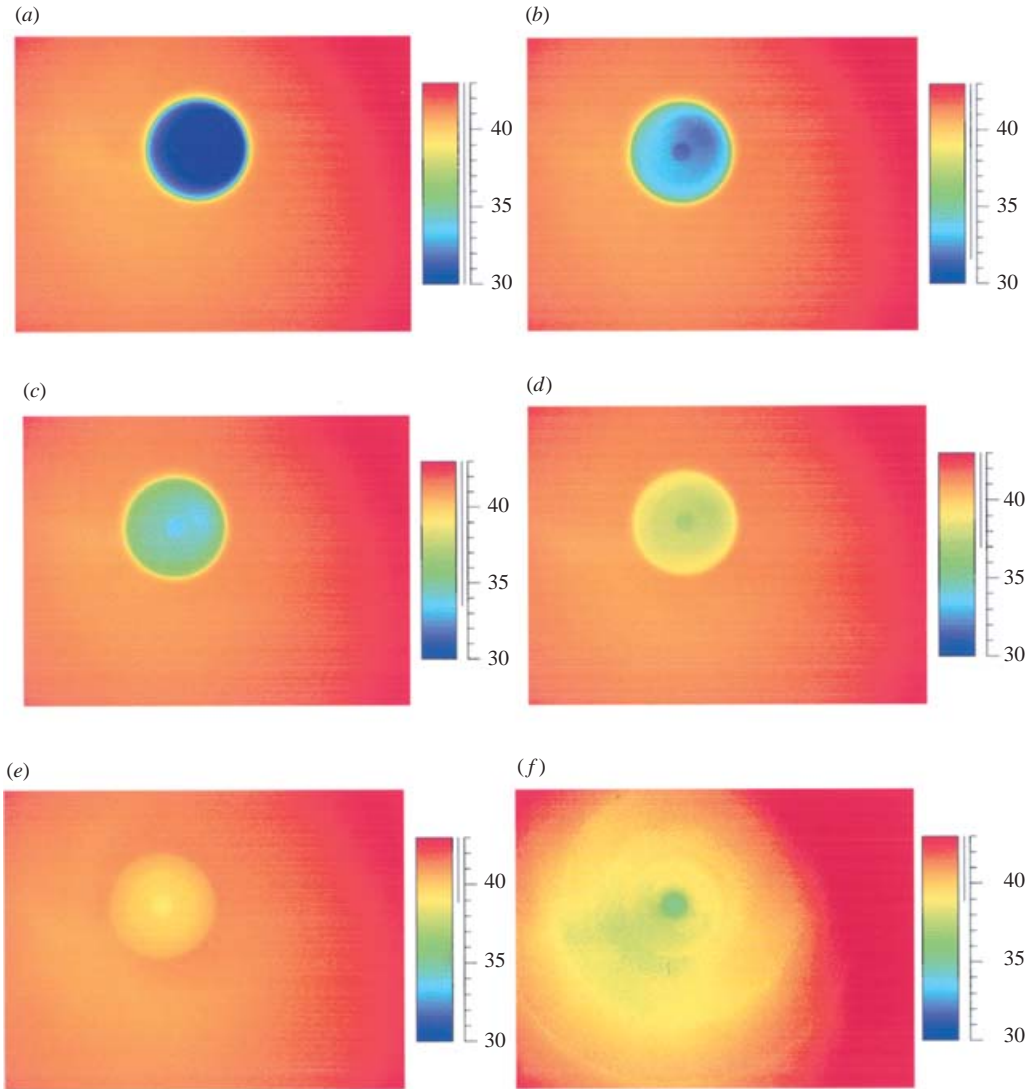


FIGURE 2. Thermographic images of a drop ($D = 3$ mm) of silicone oil with kinematic viscosity of 100 cS on a pool of silicone oil with kinematic viscosity of 3 cS. The pool temperature is 42°C , the ambient and the initial drop temperature is 25°C . (a) $t = 0$, (b) 1 s, (c) 2 s, (d) 5 s, (e) 12 s, (f) 16 s.

Figure 5 shows the measured temperature differences ($\Delta T = T_p - T_d$) between the pool and the upper surface of the droplets, for the same conditions as figures 3 and 4. The graph confirms that, as time increases, the oil drop temperature approaches the pool temperature and coalescence occurs, whereas conditions at which the water drop remains for a ‘long time’ over the pool surface are established.

Observation of the tracers’ motion on the pool surface shows that, according to previous numerical/experimental findings (Monti & Savino 1999), the flow generated at the pool surface owing to the surface tension imbalance is an inwardly directed motion towards the the cold ‘contact’ region between the spherical droplet and the pool (see discussion in §4.2).

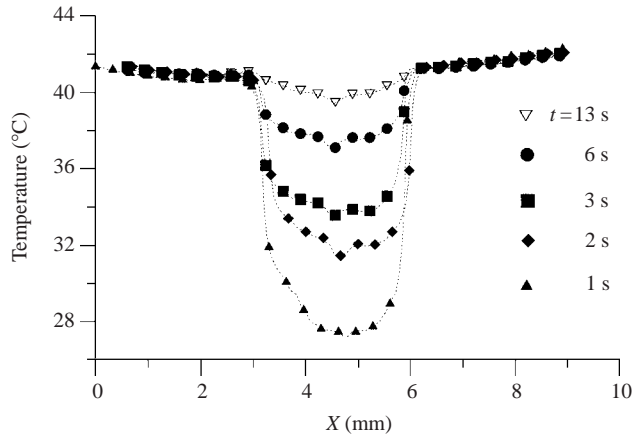


FIGURE 3. Time profiles of the surface temperature of the drop and the pool corresponding to the conditions of figure 2.

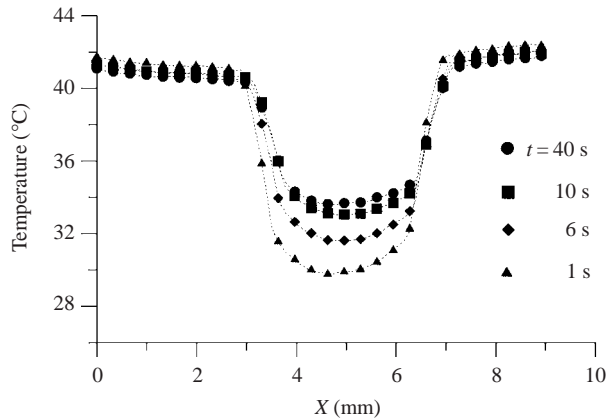


FIGURE 4. Time profiles of the surface temperature of a drop ($D = 3$ mm) of water floating over a pool of silicone oil with kinematic viscosity of 3 cS. The pool temperature is 42°C, the ambient and the initial drop temperature is 25°C.

2.3. Pool at ambient temperature

In this case, the pool liquid is at ambient temperature ($T_p = T_a \cong 25^\circ\text{C}$). The droplet temperature is initially less or greater than the pool temperature ($T_d < T_p$ or $T_d > T_p$). The main difference with respect to the situation described in §2.2 is that in this case the heat transfer between the pool and the ambient is negligible. The tests have been performed with a pool at ambient temperature (corresponding to very low vapour pressure of both water and silicone oil) to reduce evaporation effects and therefore to eliminate the possibility of a vapour film forming between the pool and the drop surface. The experiments show that if the droplet is colder than the pool ($T_d < T_p$) then the drop exhibits a behaviour similar to that described in §2.2. The drop remains floating over the pool surface until a small temperature difference is present.

If the initial temperature of the droplet is greater than the pool temperature ($T_d > T_p$), then the drop immediately coalesces (for miscible liquids) or sinks (for

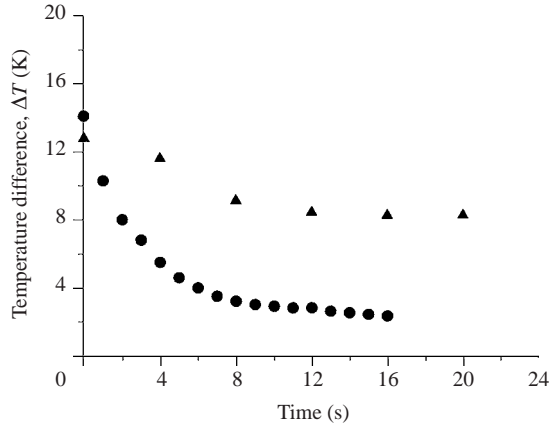


FIGURE 5. Measured temperature differences ($\Delta T = T_p - T_d$) between the pool and the droplet. The liquid pool is silicone oil with kinematic viscosity of 3 cS at a temperature $T_p = 42^\circ\text{C}$. The droplets are initially at ambient temperature ($T_a = 25^\circ\text{C}$). $D = 3$ mm. Pool: silicone oil 3 cS at $T = 42^\circ\text{C}$. \blacktriangle , water droplet; \bullet , oil droplet, 100 cS.

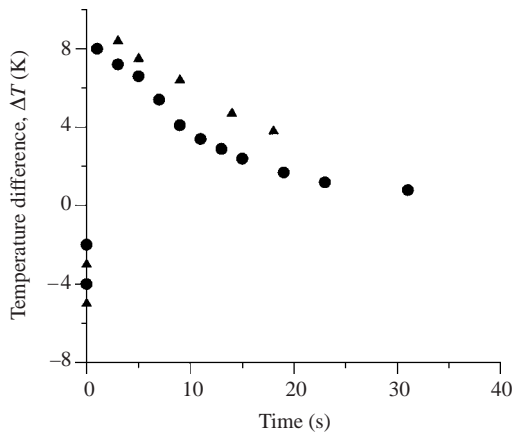


FIGURE 6. Measured temperature differences ($\Delta T = T_p - T_d$) between the pool and the droplet. The liquid pool is silicone oil with kinematic viscosity of 3 cS at ambient temperature (25°C). The droplets are initially warmer (negative temperature differences) or cooler than the ambient (positive temperature differences). In the former case, two different values of the initial temperature difference are considered. In both cases, the droplet immediately sinks (\bullet , water) or coalesces (\blacktriangle , silicone oil, 1000 cS). $D = 3$ mm.

larger density immiscible liquids), similar to the case discussed in the §2.1. Figure 6 summarizes the measured temperature differences between the pool and the upper surface of the droplet (for silicone oil 1000 cS and water). When the droplet is initially cooler than the pool ($\Delta T > 0$) it stands for a long time on the pool surface until the temperature difference decreases below a critical value (see figure 6). When the droplet is initially warmer than the pool ($\Delta T < 0$), it immediately sinks (water droplet) or immediately coalesces (silicone oil droplet). In this case, two different values of the initial temperature difference are considered both for the water and for the silicone oil droplet. In both cases, the droplet residence time is almost zero (see figure 6).

3. Explanation of the observed phenomena

Common sense suggests that the droplet would coalesce (or sink, if its density is larger than the pool liquid density); however, conditions at which the drop floats over the silicone oil pool are established owing to a temperature difference between the drop and the pool. When there is a thermal imbalance over the pool surface, creating an inward motion at the surface (because the temperature of the droplet is less than the pool surface temperature), coalescence (or sinking) is prevented by the Marangoni flows generated in the pool by the surface tension unbalance and the droplet floats for a certain time over the pool surface. This motion drags a thin film of the ambient air beneath the drop and avoids intimate molecular contact between the droplet and the oil, preventing the drop from coalescing or sinking into the pool. When the temperature difference between the oil droplet and the pool reaches a small (critical) value, then the droplet coalesces or sinks. As discussed before, the water droplet exhibits a different behaviour, because its temperature at the steady state is less than the surface temperature and conditions at which the drop floats for a 'long' time over the oil pool are established. The different behaviour of the oil and water droplets can be explained:

- (i) by the different heat capacity between the silicone oils and water;
- (ii) for the water droplets over a hot pool, evaporation may also play a role (see §4). However, as discussed in the §2.3, the tests reported in figure 6 have been performed at conditions of rather low temperatures to eliminate the possibility of a vapour film forming between the pool and the drop surface.

When the initial temperature of the droplet is greater than the pool temperature, the Marangoni flow at the pool surface is directed outward from the 'hot' contact point between the drop and the pool liquid. This motion drains the ambient air beneath the drop and allows the intimate molecular contact between the droplet and the bath, so that the silicone oil droplet immediately coalesces and the water droplet immediately sinks in the bath (figure 6).

4. Physical and numerical model

For a relatively large pool, we may assume that an axisymmetric flow field is established around the vertical axis passing through the droplet centre. The situation here is more complex when compared to the non-wetting or non-coalescence problems because in the previous cases (Monti *et al.* 1998*a, b*), the air gap was disk-shaped. In the present case, the shape of the air film depends on the pool surface deformation which is related to the droplet weight, dimension and to the liquid characteristics.

The assumption made here is that the droplet is spherical. In particular, when considering a water droplet floating on an oil bath, the silicone oil surface tension is smaller than that of the droplet water (in the ratio of 1:3.5, see table 1) so we should expect that the pool surface is not very rigid and deforms 'more' than the droplet.

The numbers that provide an idea of the order of magnitude of the two surface deformations due to a droplet of weight W and of radius R are the pool deformation factor, $\delta_p = W/\sigma_p R$, and the droplet deformation factor, $\delta_d = (W/R^2)/(2\sigma/R) = W/2\sigma R$. Another quantity that measures the surface deformation is the amount of the droplet sinking below the pool surface (h_∞) that in turn depends also on the density ratio ρ_d/ρ_p . In the subject case (droplets of $R = 0.5 - 3$ mm over a bath of silicone oil with kinematic viscosity of 3 cS), the ratio $\delta_d/\delta_p \cong O[10^{-1}]$. Consequently, we may assume, in a first approximation, that the droplet exhibits a quasi-spherical shape (this can also be seen experimentally in figure 1).

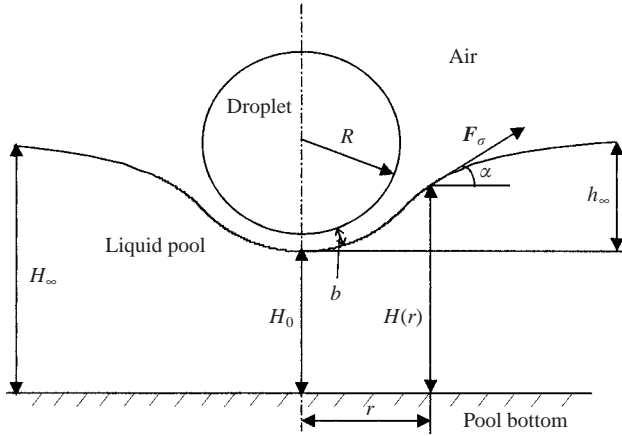


FIGURE 7. Geometry of the problem and relevant notations.

To compute the flow field in the pool, in the drop and in the ambient air (in the vicinity of the floating droplet), we must find the shape of the surface and the geometry of the air gap between the surfaces of the pool and of the drop. Analytical/numerical iteration processes, that will be illustrated in the next two subsections, are required to solve both these problems.

4.1. Surface shape computations

The proposed model geometry is depicted in figure 7. The interface shape can be evaluated by the well-known equation of Young and Laplace (Huh & Scriven 1969), which relates the difference in hydrostatic pressure across the interface to the local mean curvature and surface tension σ of the interface (see Orr, Scriven & Rivas 1975, or James 1974). For geometries with a symmetry axis, the Young–Laplace equation may be written in cylindrical coordinates to obtain the surface equation $H(r)$ (figure 7):

$$\frac{\rho g(H - H_\infty)}{\sigma} = \frac{H''}{(1 + H'^2)^{3/2}} + \frac{H'}{r(1 + H'^2)^{1/2}}. \quad (1)$$

Equation (1) can be reformulated by introducing the angle α between the local tangent to the surface and the r -axis ($\tan \alpha = H'(r)$). Then, the second-order differential equation, (1), can be replaced by two first-order equations:

$$\frac{dH}{d\alpha} = \frac{\sin \alpha}{\sin \alpha/r - \rho g(H - H_\infty)/\sigma}, \quad (2)$$

$$\frac{dr}{d\alpha} = \frac{\cos \alpha}{\sin \alpha/r - \rho g(H - H_\infty)/\sigma}. \quad (3)$$

The problem here is complicated by the fact that the sinking depth of the droplet, h_∞/R , which depends on the drop weight, is unknown.

The initial condition for (2) and (3) has been imposed taking into account the experimental observation on droplets floating on a silicone oil pool. Using a background illumination technique, the shape of the liquid pool deformed under the drop (for $r < R$) was found to be almost spherical with a radius of $R + b$ (b almost constant and of the order of $10 \mu\text{m}$). A spherical shape with the same curvature as the spherical drop has been assumed for $r/R < \xi$, where $\xi < 1$ is an unknown of the

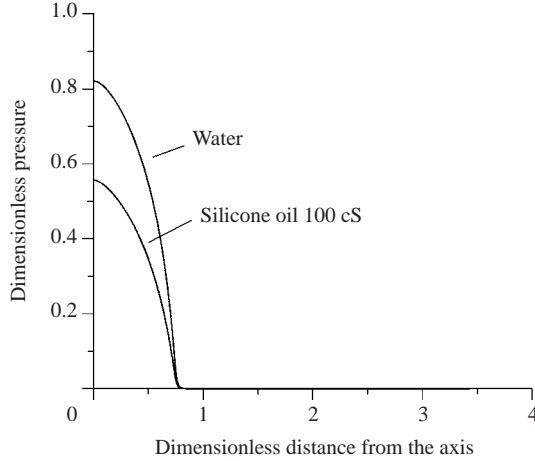


FIGURE 8. Computed pressure distribution along the pool-air interface after 5 s, for a droplet of water and a droplet of silicone oil 100 cS over a pool of silicone oil 3 cS. The film thickness is $b = 5 \mu\text{m}$. The pressure has been non-dimensionalized by ρV_m^2 , where V_m is the Marangoni velocity ($V_m = \sigma_T \Delta T / \mu$). The reference quantities correspond to the silicone oil 3 cS properties reported in table 1, and ΔT is the initial temperature difference between the drop and the pool ($\Delta T = 17 \text{K}$).

problem representing the point where the pool interface departs from the spherical shape. An iterative procedure is required to find ξ and h_∞/R . Their values have been determined by imposing the vertical equilibrium for $r > R$ (the weight of the drop (W) plus the weight of the oil contained in the volume between the free surface $H(r)$ and the pool bottom must be equal to the hydrostatic pressure force at the bottom plus the surface tension force):

$$W + \int_R^r 2\pi r H \rho_p g \, dr = \pi r^2 H_\infty \rho_p g + 2\pi r \sigma_p \sin \alpha. \quad (4)$$

Equations (2) and (3) have been solved using an Euler procedure.

The sinking depths computed taking equation (4) into account fit the corresponding experimental observations very well. Also, the pool interface shapes, as calculated for drops of different diameters, are in good agreement with the experimental shapes measured with the background illumination technique. These shapes have been considered for the numerical simulations of the thermofluiddynamic fields described in §4.2.

4.2. Thermofluiddynamic field in the drop, in the pool and in the air gap

The system of governing equations, for an incompressible flow in dimensionless form:

$$\nabla \cdot \mathbf{V} = 0, \quad (5)$$

$$\frac{\partial \mathbf{V}}{\partial t} + \mathbf{V} \cdot \nabla \mathbf{V} + \nabla p = \frac{1}{Re} \nabla^2 \mathbf{V}, \quad (6)$$

$$\frac{\partial T}{\partial t} + \mathbf{V} \cdot \nabla T = \frac{1}{Ma} \nabla^2 T, \quad (7)$$

have been solved in each phase of the flow domain, in the pool, in the drop and in the surrounding air.

In (5)–(7), \mathbf{V} is the dimensionless velocity vector, and T the dimensionless temperature. The radius of the drop is taken as the characteristic reference length; the velocity is scaled by the Marangoni speed ($\mathbf{V}_m = \sigma_T \Delta T / \mu$); μ is the dynamic viscosity, σ_T the (negative) surface tension derivative with temperature and ΔT the characteristic temperature difference; the time is scaled by R/V_m , the pressure by ρV_m^2 (where ρ is the density). The Reynolds and Marangoni numbers are defined by $Re = \rho V_m R / \mu$, $Ma = Re Pr$ (Pr is the Prandtl number). According to the experimental conditions, a constant value of 25 °C has been prescribed to the temperature on the upper boundary (corresponding to the ambient temperature), while the pool bottom wall is assumed at a constant temperature of 42 °C. The Marangoni boundary condition has been assigned on the pool–air interface, i.e.:

$$\boldsymbol{\tau} - \boldsymbol{\tau}_a = \nabla_s T \quad (8)$$

where $\boldsymbol{\tau}$ is the dimensionless shear stress in the pool, $\boldsymbol{\tau}_a$ the shear stress in the surrounding air (scaled by the viscosities ratio) and ∇_s is the dimensionless surface gradient. For silicone oil drops, the same condition (equation (8)) applies along the drop–air interface. For water droplets, the continuity of shear stresses ($\boldsymbol{\tau} = \boldsymbol{\tau}_a$) is imposed along the droplet–air interface, since the Marangoni effect is assumed to be negligible (as discussed in §2).

Numerical simulations have been performed with a Navier–Stokes code, using a finite volume method to solve the field equations. The SIMPLE (semi-implicit method for pressure-linked equations) family of algorithms (Patankar 1980) is used for introducing pressure into the continuity equation. Second-order upwind is used to discretize the momentum and energy convective fluxes. Central schemes are used for diffusive fluxes. Unsteady calculations are performed using a second-order fully implicit algorithm. Typically, the number of quadrilateral cells is of the order of 15 000 for the whole calculation.

4.3. Numerical results and correlations with experiments

Numerical results have been obtained in the case of a water droplet and of a 100 cS silicone oil droplet ($D = 3$ mm) over the 3 cS silicone oil pool, assuming that the droplets are initially at the ambient temperature ($T_a = 25$ °C]. A difficulty arises since the value of the film thickness (b) separating the floating droplet from the pool surface (see figure 7) is unknown and, during the experiment, it is not constant; this requires an iterative procedure to evaluate the time evolution of the film thickness (see §4.4).

According to the previous discussion, coalescence or sinking is prevented because air continuously feeds the film sustaining the drop, owing to the entrainment caused by the surface Marangoni velocity in the pool. Since the surface velocities are proportional to the differences of temperatures and since these differences decrease with time (see figure 5), we should conclude that the entrainment effect is reduced and the air film is drained until a critical thickness (when intermolecular forces become prevalent) is reached.

Unfortunately, experiments for the measurement of the film thickness are very difficult, but from previous numerical and experimental results (Dell’Avesana *et al.* 1997, Monti *et al.* 1998a) we can assume that for silicone oil/air/silicone oil systems coalescence is prevented for values of b above 3 μm . Therefore, a reasonable value for b has been initially assigned ($b = 5$ μm).

Figure 8 shows the calculated pressure distribution along the pool interface for the water and silicone oil droplets, at $t = 5$ s, for $b = 5$ μm . Figure 9 shows the

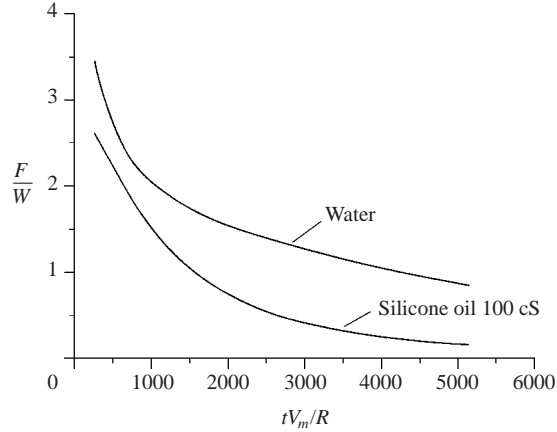


FIGURE 9. Time evolution of the force acting on droplets of water and silicone oil 100 cS, for a film thickness of $5\ \mu\text{m}$. The force F acting on the drops has been non-dimensionalized by the weight W of the water and silicone oil droplets, respectively. The time t has been non-dimensionalized by the reference time R/V_m , where R is the drop radius ($R = 1.5\ \text{mm}$) and V_m is the Marangoni velocity ($V_m = \sigma_T \Delta T / \mu$). The reference quantities correspond to the silicone oil 3 cS properties reported in table 1, and ΔT is the initial temperature difference between the drop and the pool ($\Delta T = 17\ \text{K}$).

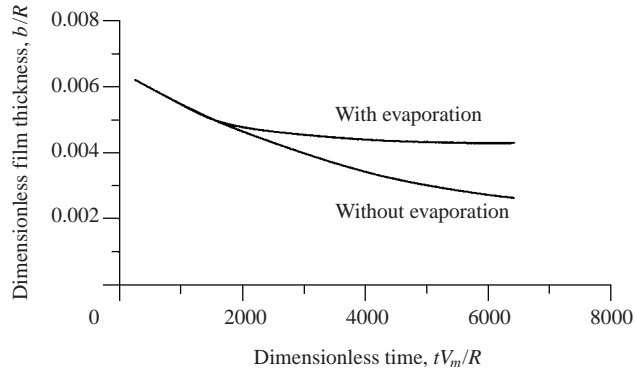


FIGURE 10. Computed time profile of the equilibrium film thickness for a water droplet ($D = 3\ \text{mm}$) at initial temperature $T_i = 25^\circ\text{C}$ floating over a silicone oil 3 cS pool at $T_p = 42^\circ\text{C}$. The two curves correspond to numerical results obtained with and without inclusion of the drop evaporation in the model.

corresponding time profiles of the forces acting on the two droplets (divided by the weight of the drop). Since the film thickness is constant with time during the calculation, the computed forces are initially larger, when the Marangoni velocities are high, and then decrease with time. However, since the sustaining force must balance the weight of the droplet at each time, it may be expected that the gap thickness b is a decreasing function of time. An extremely long and cumbersome iterative procedure has been carried out to evaluate the time evolution of the equilibrium film thickness (b), i.e. the value of b such that the computed force on the droplet, resulting from the pressures in the air gap, balances at each time the droplet weight. The computed equilibrium film thickness for the water droplet is shown in figure 10. The two curves

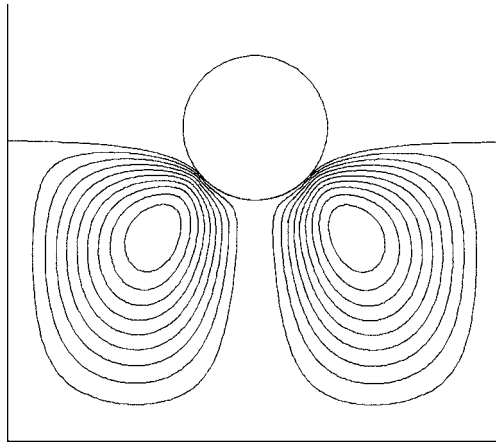


FIGURE 11. Computed streamlines in the case of a water droplet ($D = 3$ mm) over a pool of silicone oil 3 cS; the film thickness is $b = 5$ μm , $t = 5$ s. The streamfunction is non-dimensionalized by $V_m R$, where V_m is the Marangoni velocity. The maximum and minimum values of the calculated streamfunction are $\psi_{max} = 2.21 \times 10^{-5}$; $\psi_{min} = 0$. The difference between two streamlines corresponds to $\Delta\psi = 2.21 \times 10^{-6}$.

in figure 10 correspond to the calculations obtained with and without inclusion of the evaporation (see discussion below).

Figure 8 also shows that, after 5 s, the rise in the pressure, in the air film, is larger for the water droplet than for the silicone oil droplet, and this can be explained by the larger temperature differences between the water drop and the pool (see figure 5). This larger pressure gives rise to a force on the water droplet larger than that on the silicone oil droplet (see figure 9), and may explain why after about 16 s the oil droplet coalesces (see figure 3) whereas the water droplet stands indefinitely over the pool surface (figure 4).

The numerical results show that, because of the initial temperature difference between the pool and the droplet, a Marangoni flow is quickly established inside the pool (figure 11). This flow field is initially stronger and weakens gradually as the droplet and the pool approach the same temperature (i.e. the value of the maximum velocity decreases with time).

Figure 12 shows the computed velocities along the pool surface after $t = 2$ s and when steady-state conditions are established (after about 30 s), for the case of a droplet of water with diameter $D = 3$ mm. In the same graph, the velocities in the pool, measured by the tracers at the steady state, are reported for comparison.

Figure 13 shows the velocity field in the small air gap between the drop and the pool at $t = 5$ s. The Marangoni flow in the pool drags air into the gap that, by continuity, flows out of the gap near the drop interface (figure 13a). Figure 13(b) shows the flow pattern near the symmetry axis for the droplet of water. The flow in the air channel avoids the direct contact between the pool and the droplet. It determines a rise in the pressure that is responsible for the force that balances the weight of the droplet (figures 8 and 9).

The measured temperature differences between the pool and the drop are compared with the numerical results in figure 14. The agreement is fairly good for the oil droplet, whereas the water droplet data exhibit a much less satisfactory behaviour. The water droplet reaches a steady temperature which is about 9 $^{\circ}\text{C}$ less than the pool

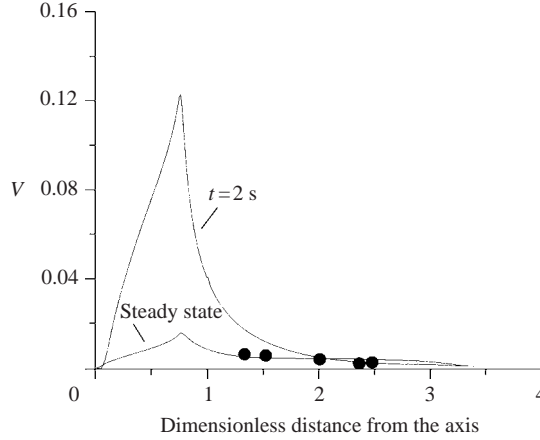


FIGURE 12. Computed velocity profiles for a water droplet ($D = 3$ mm) over a pool of silicone oil 3 cS after $t = 2$ s and after $t = 30$ s, when steady-state conditions are established. The film thickness is $b = 5$ μm ; the velocity is non-dimensionalized by the Marangoni velocity. ●, measured velocities at steady state.

temperature, whereas the results of the numerical simulations indicate that the steady-state temperature should be much closer to the pool temperature. This behaviour was explained assuming a partial evaporation of the water droplet (see discussion below). Numerical simulations including the water droplet evaporation in the model (dashed line in figure 12) show, in fact, a better agreement with the experimental data.

In this case, a uniform heat flux along the droplet surface was assumed, corresponding to an average evaporation rate $V_e = 3 \times 10^{-4}$ mm s $^{-1}$ estimated on the basis of the measured drop volume reduction (by CCD visualization). The evaporation heat flux has been evaluated as $J_e = \rho V_e H_e$, where ρ is the density of the water, V_e is the evaporation rate and H_e the latent heat of vaporization for water ($H_e = 2400$ kJ kg $^{-1}$).

4.4. Order of magnitude analysis

To find simple relationships for the physical parameters involved in the transient problem, an assessment of the orders of magnitude can be made from the energy exchange between the drop and the pool (neglecting the drop–ambient heat exchange):

$$\rho c_p V \frac{\partial T}{\partial t} = -\frac{\lambda_a (T - T_p)}{b} S, \quad (9)$$

where T is the average drop temperature, $V = \frac{4}{3}\pi R^3$ is the volume of the drop, S is the contact area between the drop and the pool (a fraction of πR^2 , i.e. $\frac{1}{4}\pi R^2$ according to the experimental configurations here investigated) ρ and c_p are the density and the specific heat coefficient of the drop, λ_a is the thermal conductivity of the air and b the film thickness.

Integration of (9) yields:

$$(T - T_p) = (T_i - T_p) \exp\left(-\frac{3\lambda_a t}{16\rho c_p R b}\right), \quad (10)$$

where T_i is the initial drop temperature. Figure 15 shows the comparison between the temperature differences computed through (10) and the numerical and experimental results, for silicone oil and water droplets.

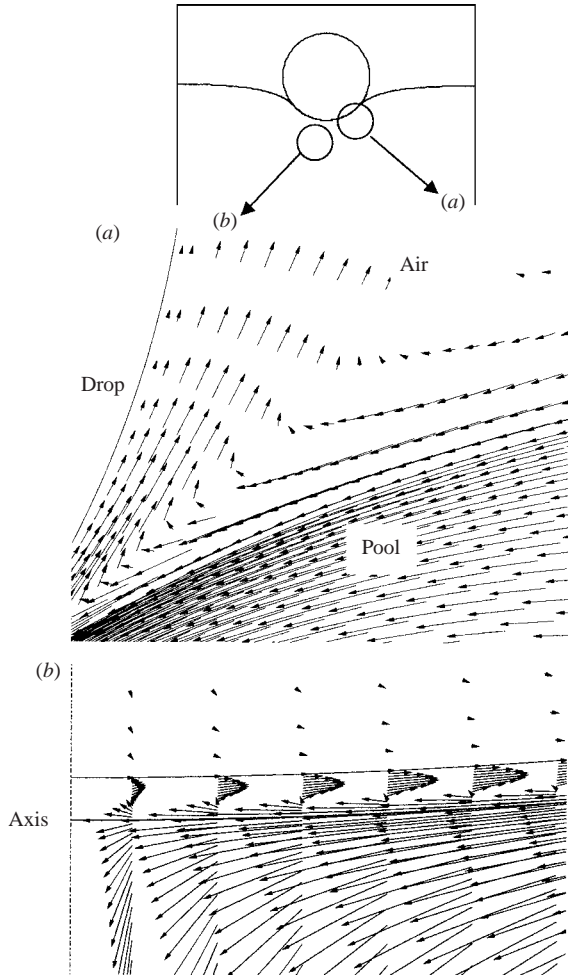


FIGURE 13. Blow-up of the velocity field in the contact region between the water droplet and the silicone oil 3 cS pool ($D = 3$ mm, film thickness $b = 5$ μm , $t = 5$ s). Dimensionless velocities, (a) $V_{max} = 0.049$; (b) $V_{max} = 0.018$.

Figure 11 indicates that, during the unsteady process, the film thickness does not change appreciably, so that a constant value (of the order of 10 μm) can be assumed under the exponential function in (10). While the agreement between the order of magnitude (OMA) analysis and the experimental and numerical results is satisfactory for the silicone oil droplet, because in this case the heat exchange between the droplet and the ambient is negligible (compared to the heat flux between the droplet and the pool), a worse correlation is found for the water droplet, since the OMA does not take into account the evaporation phenomenon.

The pressure increase in the air film, caused by the air entrainment due to the Marangoni effect along the pool surface, is of the order of magnitude of the 'lubrication' pressure in a channel of length R and thickness b :

$$\Delta p = \frac{\mu_a V_m}{b^2} R = \frac{\mu_a \sigma_T R}{\mu_p b^2} (T - T_p), \quad (11)$$

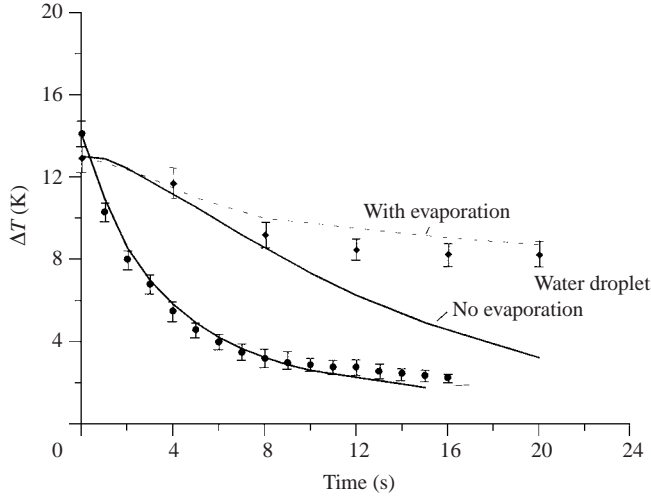


FIGURE 14. Measured temperature differences between the pool and the droplet (conditions as in figure 5) and numerical correlations (continuous curves).

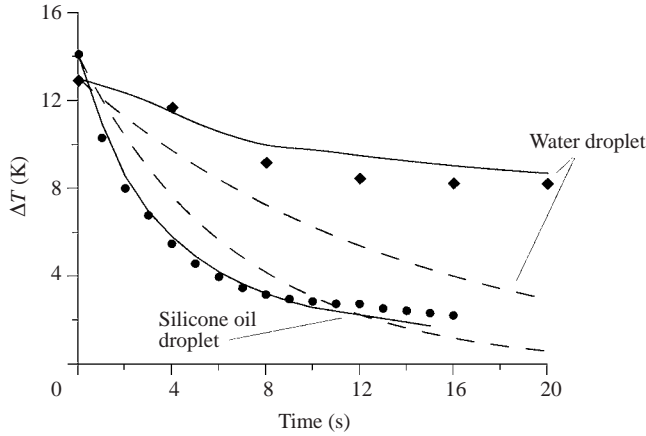


FIGURE 15. Comparison between \blacklozenge , \bullet , the experimental results, $—$, the numerical results; and $- -$, the results of the order of magnitude analysis (equation (10)) ($b = 10 \mu\text{m}$). The temperature differences are plotted versus time, for a droplet of silicone oil 100 cSt and a water droplet of $D = 3 \text{ mm}$, over a pool of silicone oil 3 cSt (pool temperature $T_p = 42^\circ\text{C}$; initial drop temperature $T_i = 25^\circ\text{C}$).

where μ_a and μ_p are the viscosities of the air and of the liquid pool, respectively, and V_m is the thermal characteristic Marangoni speed, $V_m = \sigma_T(T - T_p)/\mu_p$.

To prevent coalescence (or sinking) and allow the drop to float over the pool surface, the overall pressure force must be equal to the weight of the drop, i.e.:

$$\Delta p \frac{1}{4} \pi R^2 = \rho g \frac{4}{3} \pi R^3 \tag{12}$$

Taking into account (10), (11) and (12), we obtain an order of magnitude of the equilibrium film thickness,

$$b(t) = \sqrt{\frac{3}{16} \frac{\mu_a}{\mu_p} \frac{\sigma_T}{\rho g} (T - T_p)}, \quad (13)$$

as a function of the viscosity ratio μ_a/μ_p , and of the dynamic capillary length, $(\sigma_T/\rho g)(T - T_a)$.

Equation (14) leads to an estimation of the film thickness of the order of magnitude of $10\ \mu\text{m}$ (which is in agreement with the numerical results) for a time of the order of the duration of the experiments (about 10 s, see figure 5).

5. Conclusions

The experiments presented in this article confirm that droplet flotation is caused by the surface tension unbalance, owing to the temperature difference between the drop and the pool liquid.

The Marangoni flows generated in the pool by the surface tension gradient sustain a stable air film between the floating drop and the pool surface, thus preventing coalescence or sinking of the droplet. The results of the numerical simulations, at the experimental conditions, are in agreement with the experimental results. Laboratory tests and numerical computations are being made to consider the more intriguing and complex case of warm drops of liquids in which Marangoni effects are also present. Furthermore, the combined effects of temperature gradients and surfactants, in water solutions, will be considered in future works.

This work was partially supported by the Italian Space Agency (ASI). The authors would like to thank Professor R. Monti for helpful discussions on the subject and Professor H. Stone for a number of comments and suggestions.

REFERENCES

- ALTERIO, G. 1994 Experiments on the phenomenon of the non coalescence of two drops of silicone oil in presence of Marangoni flow. Thesis, Aeronautical Engineering, University of Naples.
- AMAROUCHE, Y., CRISTOBAL, G. & KELLAY, H. 2001 Noncoalescing drops. *Phys. Rev. Lett.* **87**, p. 206–104.
- DELL'AVERSANA, P., BANAVAR, J. R. & KOPLIK, J. 1996 Suppression of coalescence by shear and temperature gradients. *Phys. Fluids* **8**, 15–27.
- DELL'AVERSANA, P., MONTI, R. & GAETA, F. S. 1995 Marangoni flow and coalescence phenomena in microgravity. *Adv. Space Res.* **16**, 95–103.
- DELL'AVERSANA, P., & NEITZEL, P. 1998 When liquids stay dry. *Phys. Today* **51**, 38–41.
- DELL'AVERSANA, P., TONTODONATO, V. & CAROTENUTO, L. 1997 Suppression of coalescence and wetting: the shape of the interstitial film. *Phys. Fluids* **9**, 2475–2485.
- HUH, C. & SCRIVEN, L. E. 1969 *J. Colloid Interface Sci.* **30**, 323.
- JAMES, D. F. 1974 The meniscus on the outside of a small circular cylinder. *J. Fluid Mech.* **63**, 657–664.
- LAMANNA, G. 1994 Numerical simulation of the Marangoni flow in the non coalescence of two drops in microgravity conditions and correlation with experimental results. Thesis, Aeronautical Engineering, University of Naples.
- MAHAJAN, L. D. 1930a The effect of the surrounding medium on the life of floating drops. *Phil. Mag.* **10**, 383.
- MAHAJAN, L. D. 1930b Liquid drops on the same liquid surface. *Nature* **126**, 761.
- MONTI, R. & DELL'AVERSANA, P. 1994 Microgravity experimentation in non coalescing systems. *Micrograv. Q.* **4**, 123–133.
- MONTI, R. & SAVINO, R. 1996 Numerical model of non coalescing liquid drops and correlation with experimental results. *Micrograv. Q.* **6**, 102–106.

- MONTI, R. & SAVINO, R. 1997 Correlation between experimental results and numerical solutions of the Navier–Stokes problem for non-coalescing liquid drops with Marangoni effects. *Phys. Fluids* **9**, 260–263.
- MONTI, R. & SAVINO, R. 1999 Coalescence and wetting prevention by Marangoni effect. *Foams and Films* (ed. D. Weaire & J. Banhart), pp. 25–32. Springer.
- MONTI, R. & SAVINO, R. 2001 Inverse calefaction. *Naturwissenschaften* **88**, 46–48.
- MONTI, R., SAVINO, R. & CICALA, A. 1995 Surface tension-driven flow in non-coalescing liquid drops. *Acta Astronaut.* **38**, pp. 937–946.
- MONTI, R., SAVINO, R., LAPPA, M. & TEMPESTA, S. 1998a Behaviour of drops in contact with pool surfaces of different liquids. *Phys. Fluids* **10**, 2786–2796.
- MONTI, R., SAVINO, R. & TEMPESTA, S. 1998b Wetting prevention by thermal Marangoni effect. Experimental and numerical simulation. *Euro. J. Mech. B Fluids* **17**, 51–77.
- NAHMIA, J., TEPHANY, H. & MAJANELLE, P. 1997 Long life time floating drops. *J. Colloid Interface Sci.* **190**, 497–498.
- ORR, F. M., SCRIVEN, L. E. & RIVAS, A. P. 1975 Pendular rings between solids: meniscus properties and capillary force. *J. Fluid Mech.* **67**, 723–742.
- PATANKAR, S. V. 1980 *Numerical Heat Transfer and Fluid Flow*. Hemisphere.
- REYNOLDS, O. 1881 On drops floating on the surface of water. *Chem. News* **44**, 211–212.
- SAVINO, R. & MONTI, R. 1996 Modelling of non-coalescing liquid drops in the presence of thermocapillary convection. *Meccanica* **32**, 115–133.
- TEPHANY, H. & NAHMIA, J. 1999 Lifetime of floating drops under low pressure. *J. Colloid Interface Sci.* **217**, 214–215.
- WALKER, J. 1978 Drops of liquid can be made to float on the liquid. What enables them to do so?, *Sci. Am.* **238**, 151–158.